ISBN: 978-3-95450-227-1 ISSN: 2673-5490 doi:10.18429/JACoW-IPAC2022-MOPOPT067

ELECTRON BEAM PHASE SPACE RECONSTRUCTION FROM A GAS SHEET DIAGNOSTIC

N. M. Cook*, A. Diaw, C. C. Hall, RadiaSoft LLC, Boulder, CO, USA
G. Andonian, RadiaBeam Technologies, Santa Monica, CA, USA
M. Yadav, The University of Liverpool, Liverpool, UK
N. P. Norvell, The University of California Santa Cruz, Santa Cruz, CA, USA

Abstract

Next generation particle accelerators craft increasingly high brightness beams to achieve physics goals for applications ranging from colliders to free electron lasers to studies of nonperturbative QED. Such rigorous requirements on total charge and shape introduce diagnostic challenges for effectively measuring bunch parameters prior to or at interaction points. We report on the simulation and training of a non-destructive beam diagnostic capable of characterizing high intensity charged particle beams. The diagnostic consists of a tailored neutral gas curtain, electrostatic microscope, and high sensitivity camera. An incident electron beam ionizes the gas curtain, while the electrostatic microscope transports generated ions to an imaging screen. Simulations of the ionization and transport process are performed using the Warp code. Then, a neural network is trained to provide accurate estimates of the initial electron beam parameters. We present initial results for a range of beam and gas curtain parameters and comment on extensibility to other beam intensity regimes.

INTRODUCTION

Next generation accelerator facilities necessitate novel diagnostics to characterize the transverse and longitudinal profiles for ultrashort, high brightness electron beams[1]. Typical methods employ intercepting monitors such as phosphor screens, scintillators, or wire scanners[2]. These techniques are unsuitable for facilities requiring non-intercepting diagnostics, or for which beam intensities exceed damage thresholds for the requisite monitors, as well as for novel plasma-based beam sources[3]. Noninvasive gas-based monitors have been explored as residual ionization profile monitors and induced fluorescence monitors, but are limited in their sensitivity for low charge, ultrashort bunches [4, 5]. Recent work has demonstrated the viability of an intense gas column and ion transport system to provide sufficient sensitivity and resolution to meet these demands[6].

In this paper, we describe simulation studies of a non-destructive single shot diagnostic and the development of a machine learning (ML) based reconstruction algorithm capable of characterizing beam parameters from the resulting ionization measurement. The design leverages a tailored gas curtain positioned at 45° angle with respect to the incoming beam. The incident beam ionizes the gas in the curtain, and the ion products are subsequently transported and magnified through an electrostatic microscope, consisting of a triplet of annular electrostatic plates accelerating and expanding the beam until it reaches an imaging system combining a micro-channel plate detector, phosphor screen, and camera[7]. Below we describe the simulation and analysis pathway developed to describe (1) the beam-gas interaction and ionization products, (2) the transport of the ions to an imaging system, and (3) an ML-based reconstruction algorithm for determining beam parameters based on the resulting image.

BEAM-INDUCED IONIZATION

Simulations of the beam-gas interaction were performed using the Warp particle-in-cell code[8]. Warp provides support for fully self-consistent electromagnetic propagation of intense beams in two and three-dimensional geometries, as well as support for external field maps to capture an arbitrary lens configuration. Warp also includes support for several relevant ionization models. In this paper, collisional ionization was captured using a binary-electron-dipole model with relativistic corrections[9], while tunneling ionization was captured using an ADK model implementation[10]. For extremely intense beams, tunneling ionization can become the dominant mechanism, resulting in aberrations in the ion distribution consistent with the electric field profile of the beam[11]. For most of the parametric regimes under consideration for initial tests, ADK ionization rates are insignificant and impact ionization is the principal mechanism.

TRANSPORT

Beam transport through the electrostatic lens was modeled again using the Warp code along with the ion distributions generated by the electron beam and gas sheet interaction. Electrostatic fields generated from CST Microwave Studio simulations of the ion microscope were imported into Warp alongside the initial ion profile. The beam was transported 170 mm from the beam axis and magnified ~10x through the imaging plane, where a synthetic diagnostic was applied to capture the 2D profile of the beam as it would be seen on the phosphor screen. To expedite simulations, a moving window was used, and a radial aperture condition was applied to remove electrons which would otherwise collide with the electrostatic column. Figure 1 depicts a typical beam envelope as it travels along the ion microscope.

* ncook@radiasoft.net

ISBN: 978-3-95450-227-1 ISSN: 2673-5490 doi:10.18429/JACoW-IPAC2022-MOPOPT067

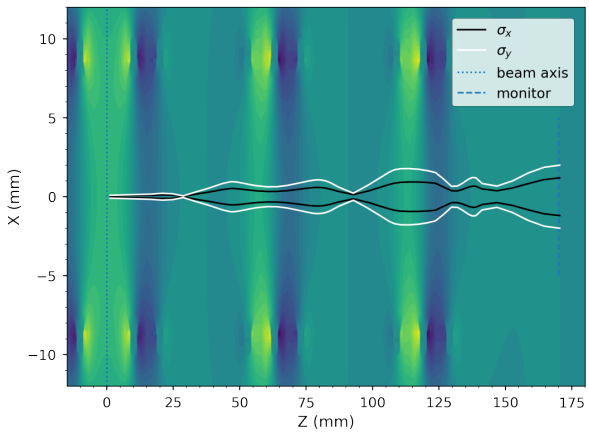

Figure 1: Simulated ion beam envelope as transported through the electrostatic lens using the Warp code.

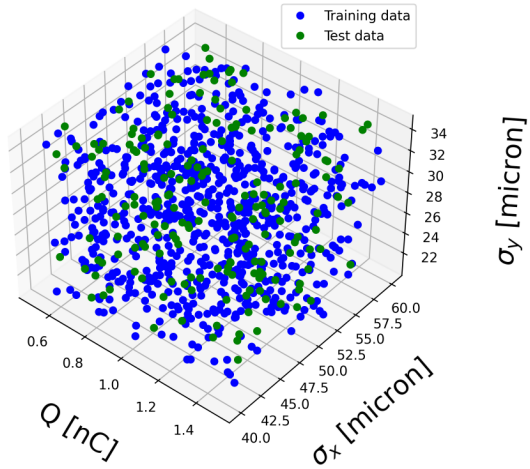

Figure 2: PIC simulations explored a three-dimensional parameter space as depicted. Test data are randomly drawn from the parameter space to obtain a 20% validation set.

RECONSTRUCTION

With the ionization and transport process models in place, we next developed a reconstruction algorithm to produce critical beam parameters using the ion image as an input.

Dataset

Our training dataset comprises input parameter settings and the corresponding output from the ionization and transport simulations, where the output is an ion image size 64×64. We performed an ensemble of large-scale Warp simulations using RadiaSoft's *rsopt* library. *rsopt* [12] is a framework designed for managing and executing resource-intensive simulations and optimizations on parallel architectures. *rsopt* enables one to decouple the optimization algorithm configuration, simulation setup, and evaluation. To support its core routines, *rsopt* is built on the libEnsemble [13, 14] library, which provides a standard API for communication between workers.

We constructed our dataset as a random subset (900 samples) of a Latin hypercube experiment design containing 1900 samples in the three-dimensional input parameter space. In order to capture the expected conditions from FACET-II, we focus on gas sheet densities in the range $10^{19}\,\mathrm{m}^{-3} \leq n_b \leq 10^{22}\,\mathrm{m}^{-3}$, a beam σ_x in the range $40\,\mu m \leq \sigma_x \leq 60\,\mu m$, and a beam σ_y in the range $20\,\mu m \leq \sigma_y \leq 35\,\mu m$. The training and testing sample points used in this study are shown in Fig. 2.

For all simulations, the beam charge was kept fixed at $Q \sim 0.5nC$, a reflection of the expected precision in beam charge delivered at the beamline for test experiments. Finally, we carried out model evaluation with a held-out 20% validation set.

Network Architecture

We employed a neural network to experimental parameters (gas sheet density, beam σ_x, and σ_y) given an image as an input. We adopted a convolutional neural network (CNN) architecture as they are convenient for processing images, and implemented our CNN in Keras [15]. The CNN comprises a sequence of 3×3 convolution layers, each applying ReLu activation and batch normalization. A dropout of 0.25 is applied between layers and a dense layer (128) is employed after the final convolution. We employ a conventional formulation based on minimizing a loss function with the mean-squared error. We minimize this output by accelerated gradient descent using an Adam optimizer with a learning rate set to $lr = 10^{-3}$ in a series of *epochs*. We employed the *ReLu* activation function and *MinMaxScaler* regularization. Input images were downsampled to 64×64 arrays to reduce network size and expedite training. Figure 3 depicts an example reconstruction from a sample ion beam image to an electron transverse beam trace space.

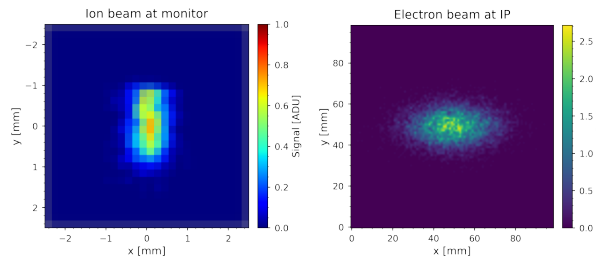

(a) Simulated ion image (b) Reconstructed e^- beam

Figure 3: Example reconstruction.

Results

Figure 5 illustrates the training and validation loss error. The loss error goes down up to 100 epochs, reaching a plateau for both the training and validation curves. We do not see any prior indication of potential overfitting.

Figure 4 show the correlation plots with the test score for the sheet density, beam σ_x, and beam σ_y. We observe that the determination coefficient R^2 converges towards 1.0 for each parameter, indicating that the surrogate model accu-

ISBN: 978-3-95450-227-1 ISSN: 2673-5490 doi:10.18429/JACoW-IPAC2022-MOPOPT067

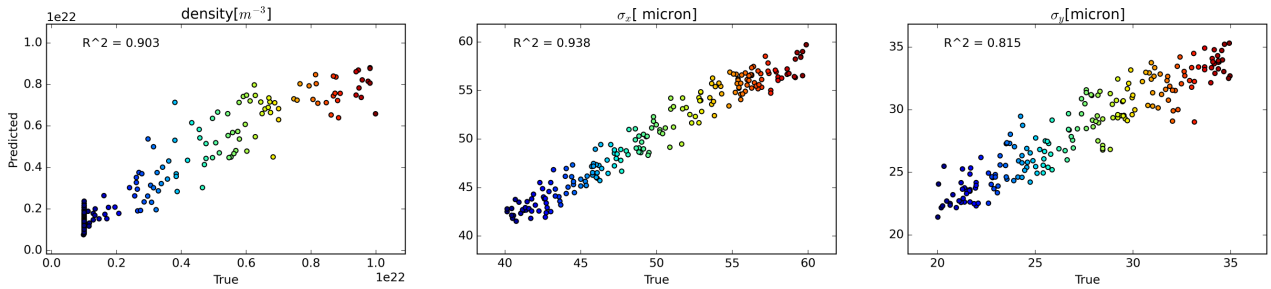

Figure 4: Performance test of the candidates surrogate learned with the CNN. From left to right, subpanels depict the sheet density, beam σ_x, and beam σ_y. The x-axis depicts data from the Warp simulations (true representation); the y-axis represents the surrogate model prediction. Note that the CNN surrogate reproduces truth representation relatively well in each case, and the coefficient of determination R^2 for each variable exceeds 0.8, indicating the robustness of the prediction.

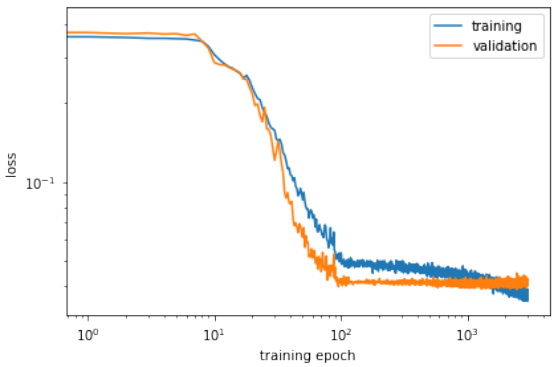

Figure 5: Training and validation loss as function of epoch follow closely, indicating no overfitting in this regime.

rately represents the ground truth data. Our relatively simple CNN model struggles to predict the charge distribution when including the beam charge as a fourth input parameter to the space. One may expect that a better sampling strategy that efficiently covers input space may help improve the model performance. Additionally, tuning the CNN's optimizer, termination conditions, and other hyperparameters will likely produce a better model.

CONCLUSION

We have designed and modeled a non-destructive single-shot diagnostic for high brightness electron beams. The diagnostic leverages a low density gas sheet, electrostatic ion microscope, and high gain imaging system to control and amplify a precision ionization signal. We simulated the electron beam interaction with the gas sheet, evaluated the ionization products, and transported the ions through the electrostatic column to generate an emulated image. We then developed and trained a neural network to reproduce critical beam parameters such as charge and transverse profile using only the resulting image as an input. The resulting network robustly identifies beam parameters across a 50% variation in beam transverse size, and an order of magnitude variation in gas sheet density. Furthermore, the evaluation of the neural network is orders-of-magnitude faster than the execution of the series of PIC simulations. This work demonstrates the efficacy of both the diagnostic design and of ML-based analysis to predict beam parameters at unprecedented brightness.

ACKNOWLEDGMENTS

This material is based upon work supported by the U.S. Department of Energy, Office of Science, Office of High Energy Physics under Award Number DE-SC0019717.

REFERENCES

[1] V. Yakimenko *et al.*, "Facet-ii facility for advanced accelerator experimental tests," *Phys. Rev. Accel. Beams*, vol. 22, p. 101 301, 10 2019, doi:10.1103/PhysRevAccelBeams.22.101301

[2] M. G. Minty and F. Zimmermann, *Measurement and control of charged particle beams*. Springer, 2003, doi:10.1007/978-3-662-08581-3

[3] A. Cianchi *et al.*, "Challenges in plasma and laser wakefield accelerated beams diagnostic," *Nuclear Instruments and Methods in Physics Research Section A: Accelerators, Spectrometers, Detectors and Associated Equipment*, vol. 720, pp. 153–156, 2013, Selected papers from the 2nd International Conference Frontiers in Diagnostic Technologies (ICFDT2), doi:https://doi.org/10.1016/j.nima.2012.12.012

[4] I. Yamada, M. Wada, K. Moriya, J. Kamiya, P. K. Saha, and M. Kinsho, "High-intensity beam profile measurement using a gas sheet monitor by beam induced fluorescence detection," *Phys. Rev. Accel. Beams*, vol. 24, p. 042 801, 4 2021, doi:10.1103/PhysRevAccelBeams.24.042801

[5] A. Salehilashkajani *et al.*, "A gas curtain beam profile monitor using beam induced fluorescence for high intensity charged particle beams," *Applied Physics Letters*, vol. 120, no. 17, p. 174 101, 2022, doi:10.1063/5.0085491

[6] V. Tzoganis, H. D. Zhang, A. Jeff, and C. P. Welsch, "Design and first operation of a supersonic gas jet based beam profile monitor," *Phys. Rev. Accel. Beams*, vol. 20, p. 062 801, 6 2017, doi:10.1103/PhysRevAccelBeams.20.062801

[7] N. Norvell *et al.*, "Gas Sheet Ionization Diagnostic for High Intensity Electron Beams," in *Proc. IPAC'21*, Campinas, SP, Brazil, 2021, paper MOPAB140, pp. 489–491, doi:10.18429/JACoW-IPAC2021-MOPAB140

[8] J.-L. Vay, D. P. Grote, R. H. Cohen, and A. Friedman, "Novel methods in the particle-in-cell accelerator code-framework warp," *Computational Science &amp Discovery*, vol. 5, no. 1, p. 014 019, 2012, doi:10.1088/1749-4699/5/1/014019

ISBN: 978-3-95450-227-1 ISSN: 2673-5490 doi:10.18429/JACoW-IPAC2022-MOPOPT067

[9] Y.-K. Kim, J. P. Santos, and F. Parente, "Extension of the binary-encounter-dipole model to relativistic incident electrons," *Phys. Rev. A*, vol. 62, p. 052 710, 5 2000, doi:10.1103/PhysRevA.62.052710

[10] M. Chen *et al.*, "Numerical modeling of laser tunneling ionization in explicit particle-in-cell codes," *Journal of Computational Physics*, vol. 236, pp. 220–228, 2013. doi:10.1016/j.jcp.2012.11.029

[11] R. Tarkeshian *et al.*, "Transverse space-charge field-induced plasma dynamics for ultraintense electron-beam characterization," *Phys. Rev. X*, vol. 8, p. 021 039, 2 2018, doi:10.1103/PhysRevX.8.021039

[12] C. Hall, *Rsopt: Python framework for testing and running black box optimization problems*, https://github.com/radiasoft/rsopt, 2020.

[13] S. Hudson, J. Larson, S. M. Wild, D. Bindel, and J.-L. Navarro, "libEnsemble users manual," Argonne National Laboratory, Tech. Rep. Revision 0.8.0, 2021, https://buildmedia.readthedocs.org/media/pdf/libensemble/latest/libensemble.pdf

[14] S. Hudson, J. Larson, J.-L. Navarro, and S. Wild, "libEnsemble: A library to coordinate the concurrent evaluation of dynamic ensembles of calculations," *IEEE Transactions on Parallel and Distributed Systems*, vol. 33, no. 4, pp. 977–988, 2022, doi:10.1109/tpds.2021.3082815

[15] F. Chollet *et al.*, *Keras: The Python Deep Learning library*, Astrophysics Source Code Library, record ascl:1806.022, 2018.